MODELLING OF THE HYDRODYNAMICS IN SØRVÁGSFJØRÐUR TO SUPPORT SIMULATION OF RELATED FISH FARMING PROCESSES

Prepared by
Gerhardus Diedericks and Gunnvør á Norði

June 2022

Contact details:

Dr Gerhardus Diedericks, Stellenbosch University, Department of Mathematical Sciences, Division of Applied Mathematics, Private Bag X1, Matieland 7602
E-mail: hardus@sun.ac.za

Dr Gunnvør á Norði, Fiskaaling, Aquaculture Research Station of the Faroes, Department of Ecology, við Áir 11, 430 Hvalvík
E-mail: gunnvor@fiskaaling.fo

Acknowledgements:

AquaVitae, grant agreement no. 818173
Prof Neill Goosen

Contents

1. Introduction

1.1 Background

In the design and management of fish farms it is standard practice to measure currents and waves at one or two locations near the fish farm. A dispersion model is then used to assess the dispersion of effluents at the farm (Cromey, 2002). In this kind of dispersion modelling the measured currents are used and it is assumed that the currents are spatially uniform in the farm area. Three-dimensional hydrodynamic modelling (that can also account for dispersion) is generally not conducted since it is tedious, time consuming and requires specialist hydrodynamic modelling software and modellers. However, some studies have been conducted to compare the predicted dispersion from these three-dimensional models to the standard dispersion models (Symonds, 2011; Bannister et al, 2016). In this study, a three-dimensional hydrodynamic model is set up with the main objective to determine the degree of variability of currents in and around a fish farm. Another process that is also simulated as part of the hydrodynamic modelling is the salinity and consequently the water density. Although not directly addressed in this study, it is also possible to model the water temperature, the dispersion of farms wastes (uneaten food and faeces) and surface drifters (lice and viruses).

The site that has been selected for the study is a fish farm located within the Sørvágsfjørður in the Faroe Islands. For the site, there are measurements of water levels at a point as well as measurements of water velocity through the depth at a point and also cross-sectional velocity measurements along transects. In addition, there are also temperature and salinity measurements available at a point through the depth.

1.2 Objectives and structure of the report

The main objective of the study is to set up a three-dimensional hydrodynamic model of Sørvágsfjørður in the Faroe Islands. It will be investigated what information and data are required to set up a model that includes the main features or processes within the fjord. It will also be determined what information is required to calibrate the model. By considering the variability of the currents it will then be possible to assess the advantages of having three-dimensional hydrodynamics of the fjord compared to assuming the currents to be uniform.

The main objectives of this study are therefore:

- To evaluate the feasibility to set up a three-dimensional hydrodynamic model of Sørvágsfjørður and to determine what information is required to calibrate the model.
- To evaluate if the model can be used to simulate farming related processes. These may not be done directly, but only the feasibility determined.

Chapter 2 of this report describes the approach adopted as well as the general oceanography of the area. In Chapter 3 the model is discussed as well as the data that is included in the model and the model results. Some conclusions are drawn in Chapter 4.

2. Study approach

2.1 Physical features and oceanography

The Faroe Islands are an archipelago of 18 mountainous islands that are located halfway between Scotland and Iceland in the Northern Atlantic. The Faroe Islands are situated on the Faroe Plateau which has a local shelf around it to a depth of about 500 m (Hansen et al. (2003). The size of the shelf, where depths are less than 120 m covers an approximate area of about 10 000 km^2. It is separated from other shallow areas by depths exceeding 400 m in all directions. Below 500 m, cold deep Norwegian Sea water dominates. The upper layers, above 500 m depth, are dominated by Atlantic water from the North Atlantic Current which flows north-easterly (Steingrund and Gaard, 2005).

There is a closed clockwise circulation around the Faroe Islands on the shelf (Hansen et al., 2017). According to Steingrund and Gaard (2005) on the Faroe Shelf, extremely strong tidal currents lead to intense mixing of the water column, resulting in homogeneous water masses in the shallow shelf areas. The well-mixed shelf water is separated relatively well from the offshore water by a persistent tidal front, which surrounds the shelf at about the 100 to 130 m bottom depth contour. In addition, residual currents have a persistent clockwise circulation around the islands. These circulation patters lead to a relatively uniform shelf ecosystem on the Faroe Shelf that is different from the offshore environment. Steingrund and Gaard (2005) also concluded that the salinity is always somewhat less on the Faroe Shelf than in the surrounding ocean and the front between the oceanic and shelf water follows the bottom contour and is generally situated between the 100 m to 150 m isobaths. For the area between Sørvágsfjørður and Mykines to offshore of Mykines they list salinity values between 35.17 and 35.19.

The marine ecosystems around the Faroe Islands are highly productive with a diversity and abundance of marine species. In particular, the inflow of warm Atlantic waters to the northern seas, often called the Gulf Stream, is one of the most important factors for the ecosystem in the region. The clean, temperate waters and strong currents around the islands provide ideal conditions for fish farming. The farming of Atlantic salmon and rainbow trout is an important and growing part of the total Faroese fish production. The properties of the Atlantic water as it flows through the Faroe area are a necessary factor in any study of the climate and living conditions in the Nordic Seas and adjacent shelf seas (Larsen et al., 2012).

2.2 Local hydrodynamics

The flow within Sørvágsfjørður has been measured by á Norði and Patursson (2017) at different transects across the fjord and also at a single fixed mooring. According to the measurements, the circulation is driven by the freshwater runoff from land that causes the upper layer of water to flow out of the fjord while the denser water from outside the fjord is entrained into the fjord at depth. Furthermore, the Coriolis force tends to push the water to the right of the flow direction and therefore inflow takes place mostly along the southern side of the fjord with outflow dominating the northern side.

The mooring station where the current measurements were taken with an ADCP is located along the southern side of the fjord near the fish farm. The measured current data is very detailed and was smoothed by taking a 30-minute running average. The current speeds at different depths are presented in Figure 2.1 with the directions given in Figure 2.2. It is evident that the surface currents (50.15 m from the bottom) are substantially higher than the rest of the currents through the depth. Interestingly, the currents near the bottom are of similar magnitudes as the currents at mid-depth and at times even higher. It is also useful to investigated to what extent the currents are influenced by wind. The currents at the three surface bins are shown in Figure 2.3 together with the wind speed. The currents and wind from the Glyvursnes wind station that fall in the range from 0 to 180 degrees are considered to be directed into the fjord (and are indicated by positive values in Figure 2.3) whereas currents and winds in the range from 181 to 360 degrees are directed out for the fjord (and are indicated by negative values in Figure 2.3). As reflected in Figure 2.3, the current directions of the two top bins (50.15 m and 46.14 m from the bottom) are similar and do not follow the currents at the next bin (42.15 m from the bottom). It also seems as if the flow in the two top bins follow the wind direction more closely than the bin at 42.15 m. Similarly to á Norði and Patursson (2017), it can be seen that the wind influences the current directions up to a depth of about 5 metres.

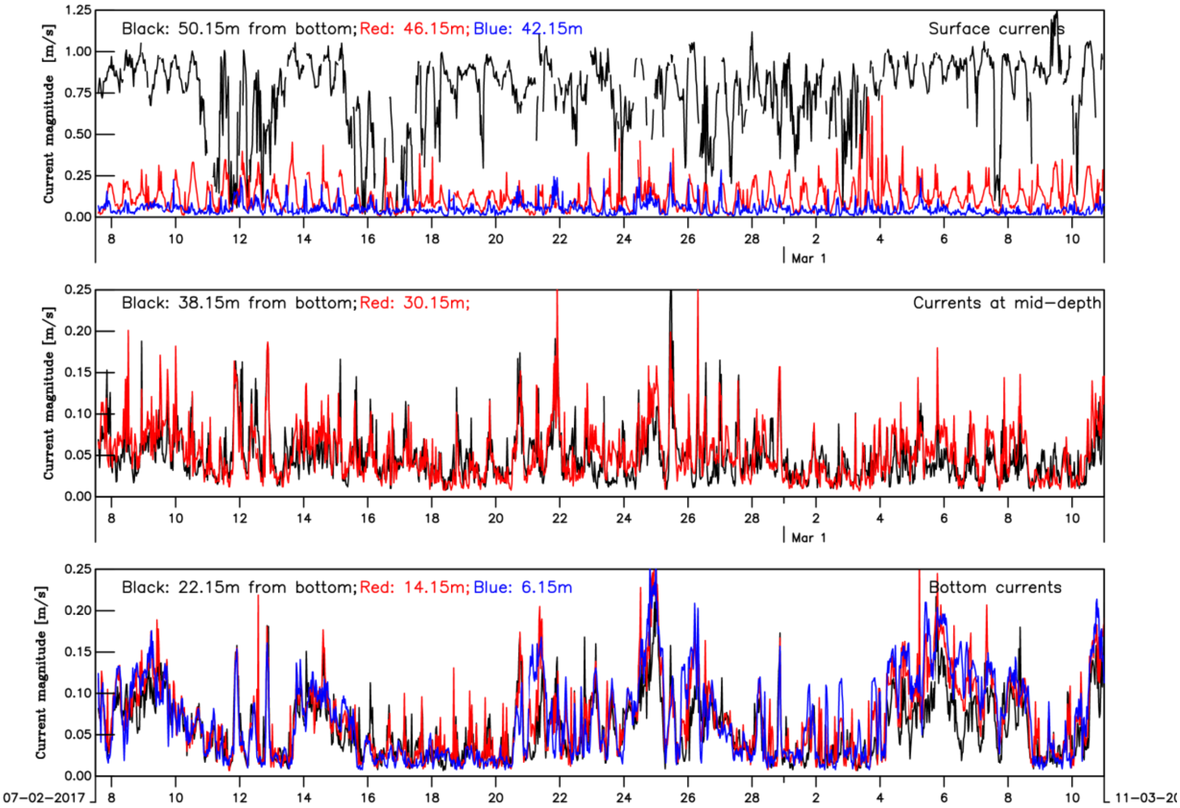

Figure 2.1 Measured current speeds at different depths at the fixed ADCP location.

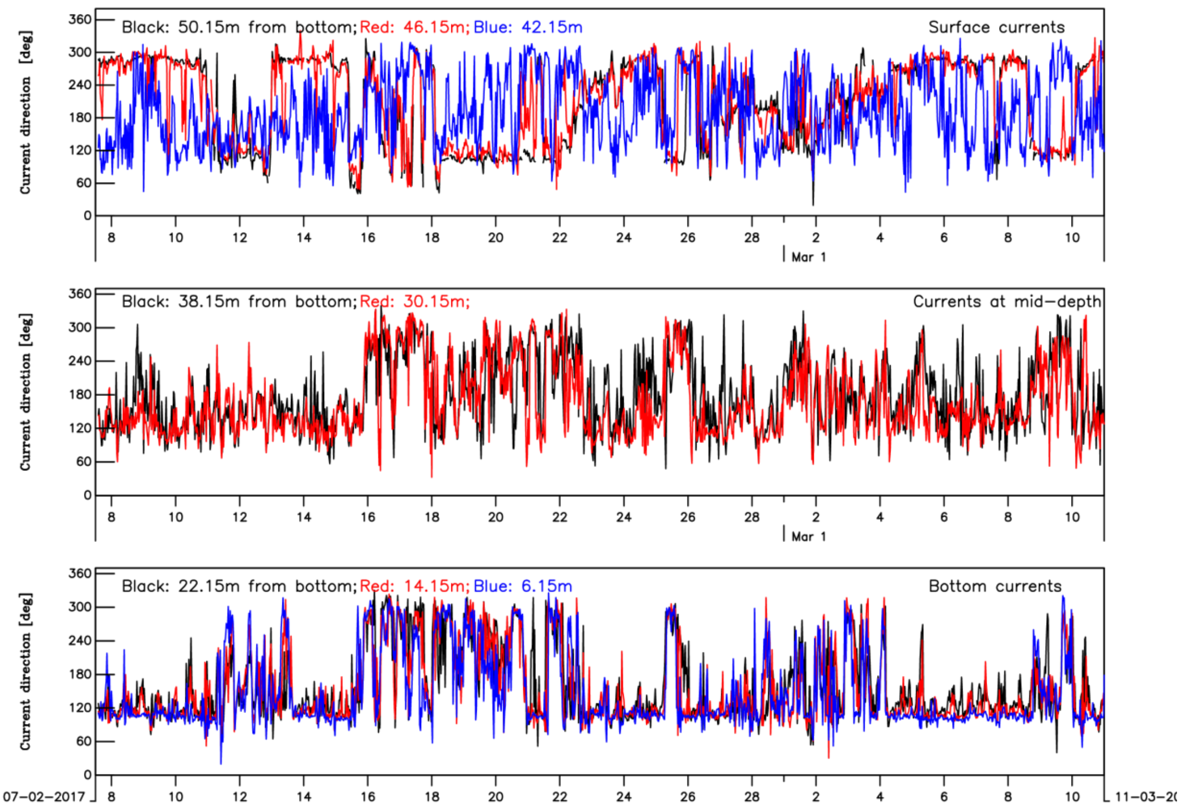

Figure 2.2 Measured current directions at different depths at the fixed ADCP location.

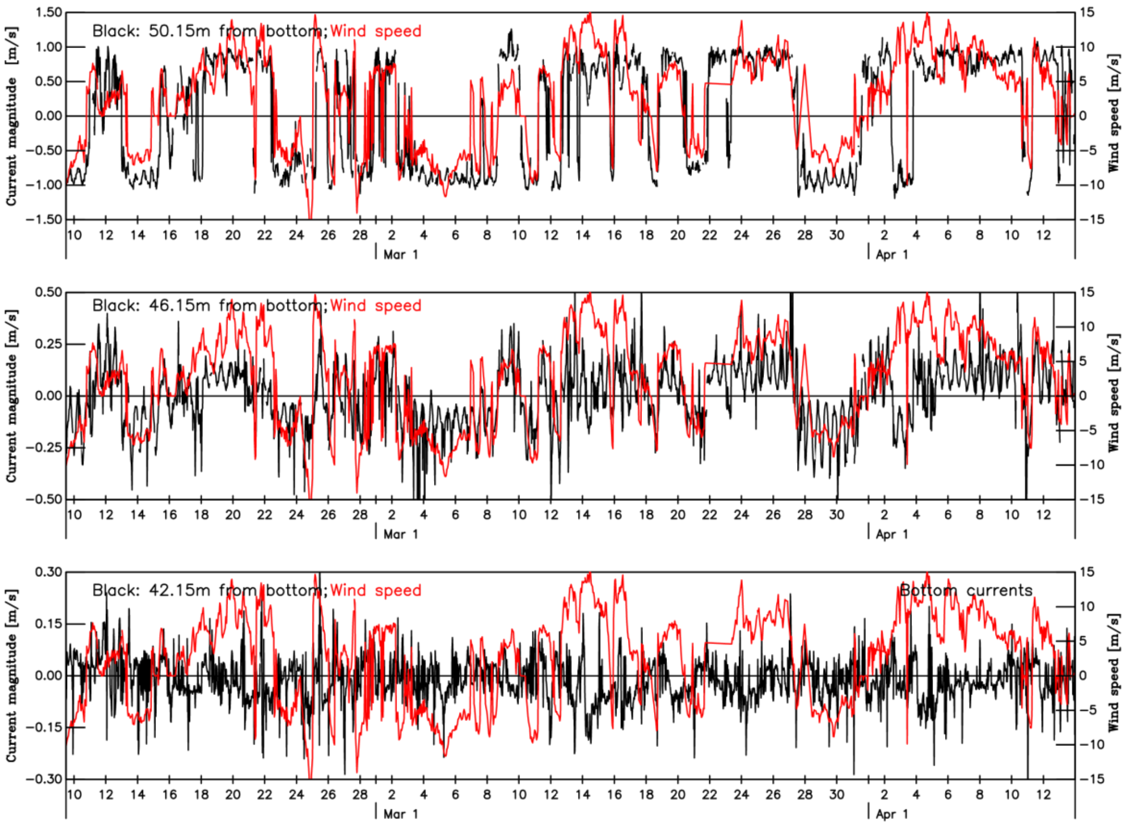

Figure 2.3 Measured currents and wind from the Glyvursnes station. Positive values indicate flow and wind into the fjord and negative values indicate flow and wind out of the fjord.

á Norði and Patursson (2017) also indicated that reverse circulation where currents are directed into the fjord occurs but that it cannot be sustained indefinitely due to the accumulation of lighter surface water in the fjord. On the other hand, with winds blowing out of the fjord, estuarine circulation with surface currents out of the fjord and inwards currents in the deeper water was observed.

2.3 Methodology

From the discussion about the hydrodynamics of the fjord, it is evident that it is necessary to set up a three-dimensional model since the flow has different directions and salinities through the depth. Wind is important since it influences the surface currents and it is also necessary to include freshwater runoff. To assess the three-dimensional currents in Sørvágsfjørður, the following steps are followed:

- A three-dimensional model will be set up that extends beyond the immediate confines of Sørvágsfjørður for in case it becomes necessary to include wider oceanographic processes into the modelling.
- The offshore tidal components and oceanic salinities will be assessed and specified as model boundary information. In this regard, the offshore model domain will be restricted to depths less than 200 m.
- It can be expected that the wind directions within the fjord may be influenced by the local topography and be directed along the main axis of the fjord. Winds that are representative of winds in the fjord will be used at the fjord while different winds will be specified for the offshore part of the model.
- Freshwater runoff from the catchments that provides runoff into the fjord need to be included in the model.
- The modelled currents and salinities will be compared to measurements. In the initial modelling, no attempt will be made to calibrate the model, but the model results will only be compared to the measurements to ascertain its feasibility to be used as basis for other modelling. If deemed necessary, a calibration process will be followed.

The methodology can be further extended once the basic processes are included and if it is deemed necessary. Additional changes may include the specification of space and time varying wind speeds and air pressures as well the inclusion of air-sea interactions. This will only be necessary if the water temperature is also modelled. There are also some model parameters such as those for the turbulence modelling and bottom friction that may be changed as part of a calibration process. If the specification of the tidal constituents is inadequate, then the boundaries can be improved by specifying so-called Riemann invariants.

3. Hydrodynamic modelling

The simulation software that is used is Delft3D-FLOW which is part of the Delft3D suite of models developed by Deltares in the Netherlands over the last three decades (Deltares, 2010; Lesser et al., 2004). The version used in this study allows for modelling by means of curvilinear grids that allows for domain decomposition. This implies that two or more models are set up and these are executed simultaneously, each providing boundary information to the other. In the present modelling, two Delft3D-FLOW models are used and they are connected via domain decomposition. Over the last few years, a major change to the software is to use unstructured grids that are associated with a flexible mesh model referred to as Delft3D-FM. It is uncertain to what extent all processes are robustly included and tested in Delft3D-FM and whether domain decomposition is supported. Therefore, the grids are set up such that the modelling will be conducted with the curvilinear model since this reduces the risk of simulating processes for which there are limited validation with the Delft3D-FM model.

3.1 The numerical model Delft3D-FLOW

3.1.1 Description

The Delft3D suite contains modules (or models) that can simulate waves, hydrodynamics, sediment transport and water quality. Delft3D-FLOW is a three-dimensional, finite volume hydrodynamic and transport model which simulates flow and transport resulting from tidal and meteorological forcing. In the present application, each of the two hydrodynamic models solves the Navier-Stokes shallow water equations with hydrostatic and Boussinesq approximations (Deltares, 2010; Lesser et al., 2004), the continuity equation, the equation of state and the advection-diffusion equation for heat, salt and sediments which are solved using the Alternating Direct Implicit (ADI) scheme. Vertical turbulence is modelled using the k-ε turbulence closure model. The model includes formulations and equations that take into account the following processes:

- tidal forcing;
- wind forcing;
- wave forcing;
- baroclinic currents and vertical mixing induced by changes in water temperature resulting from both advection of warmer/cooler water as well as local air-sea interactions;
- the effect of the earth's rotation (Coriolis force).

All these processes were included in the present model except wave forcing. The computational grid is an irregularly-spaced, orthogonal grid in the horizontal and a sigma-coordinate grid in the vertical. The equations and their numerical implementation are described in detail in Deltares (2010) and a clear exposition is also presented by Lesser et al. (2004).

An advantage of using the Delft3D-FLOW model is that when it performs the hydrodynamic computations it simultaneously calculates the transport constituents like temperature and salinity as well cohesive (mud) and non-cohesive (sand) sediment fractions.

3.1.2 Model set-up: Computational grids and bathymetry

The bathymetry of the wider area around Sørvágsfjørður which is used in the outer model, is presented in Figure 3.1 with a more detailed view of the bathymetry of Sørvágsfjørður used for the high-resolution inner model, provided in Figure 3.2. The bathymetry was provided as contours at 10 m resolution to a depth of 170 m which covered the large outer area as well as some of the channels between the islands. The depth contours in the fjord were provided at a resolution of 10 to 20 m. The measurements were conducted as single beam measurements by Landsverk and are available at www.kortal.fo. The datum level of the depths is unknown, but the depths were adjusted by 2.25 m during the modelling to get the modelled and measured water depths to be the same at the measurement location within the fjord.

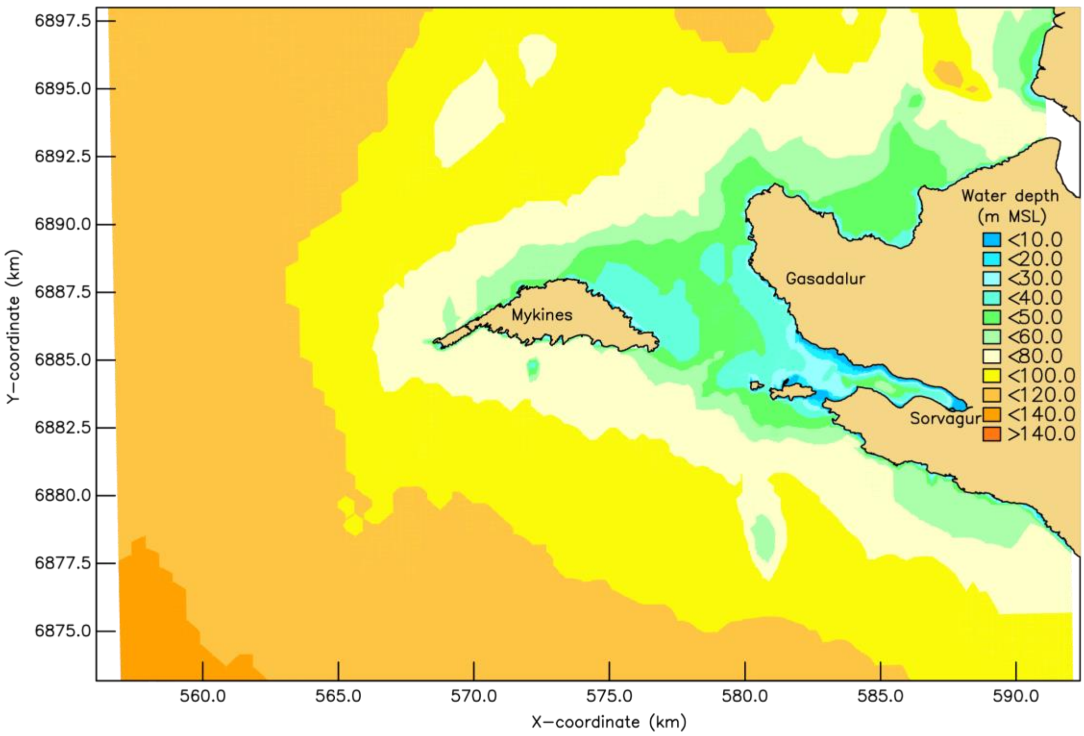

Figure 3.1 The bathymetry of the overall modelling domain.

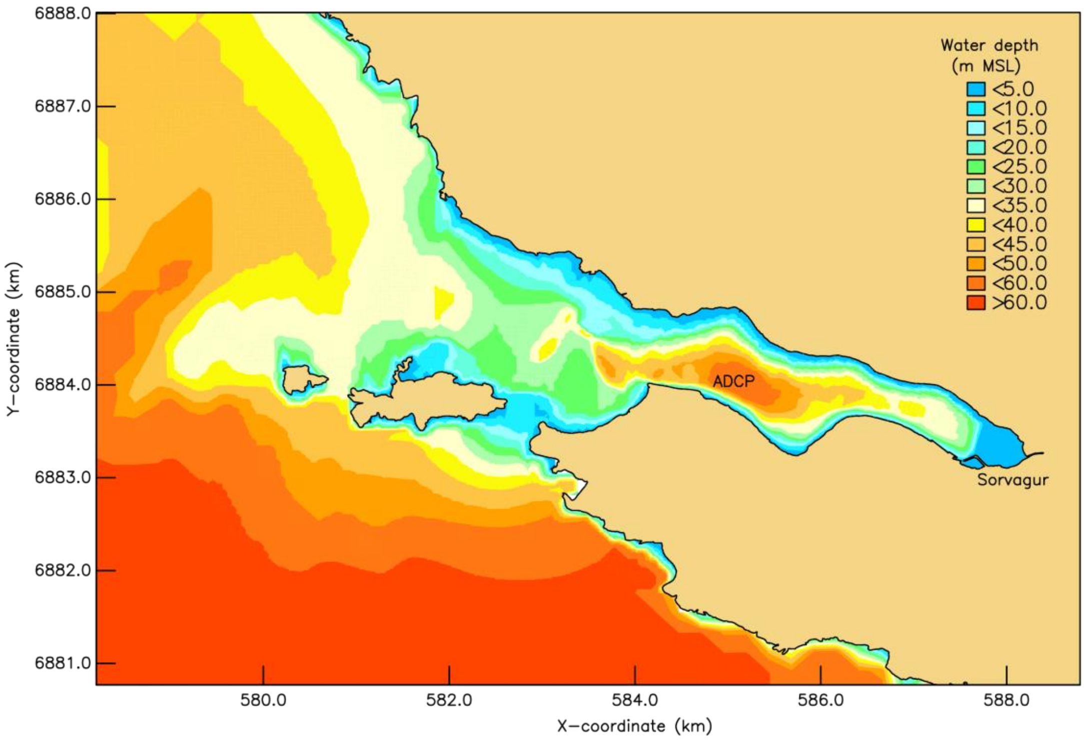

Figure 3.2 The bathymetry of Sørvágsfjørður and the location of the measurement location (ADCP).

The coordinate system used in the model is a spherical coordinate system that gives the latitude and longitude of points on the Earth. Figures 3.1 to 3.4 are presented in UTM coordinates for display purposes only. The bathymetry data was relative to an unknown level and was adjusted to correspond to the depth at the measurement location and it is expected that this positioned the bathymetry relative to mean sea level.

The entrance to Sørvágsfjørður has small islands on the south-western side and a channel offshore of the fjord between the main island and the island of Mykines. The flow at the entrance to the fjord may be rather complicated and setting up boundaries proved to be difficult. In future, it may be necessary to extend the modelling beyond local hydrodynamics (water levels and current velocities) and salinity and to also include mesoscale effects as well as temperature. It was therefore decided to make a large horizontal grid with fairly low resolution that extends approximately 15 km to the north and south of the fjord and 25 km offshore as shown in Figure 3.3. The deepest part of this grid is in the south-west at a depth of 135 m. A second high resolution horizontal grid that extends 3 km offshore was made for the fjord that includes the islands on the south-western side and is as shown in Figure 3.4. The models corresponding to each of these two grids are connected with domain decomposition. The larger outer grid has 11603 cells that vary in size from 500 m by 500 m to 250 m by 250 m while the inner grid for the fjord has 13011 grid cells with an average size of about 50 m by 50 m. The grids are designed in spherical coordinates. There are 10 equally spaced sigma layers in the vertical.

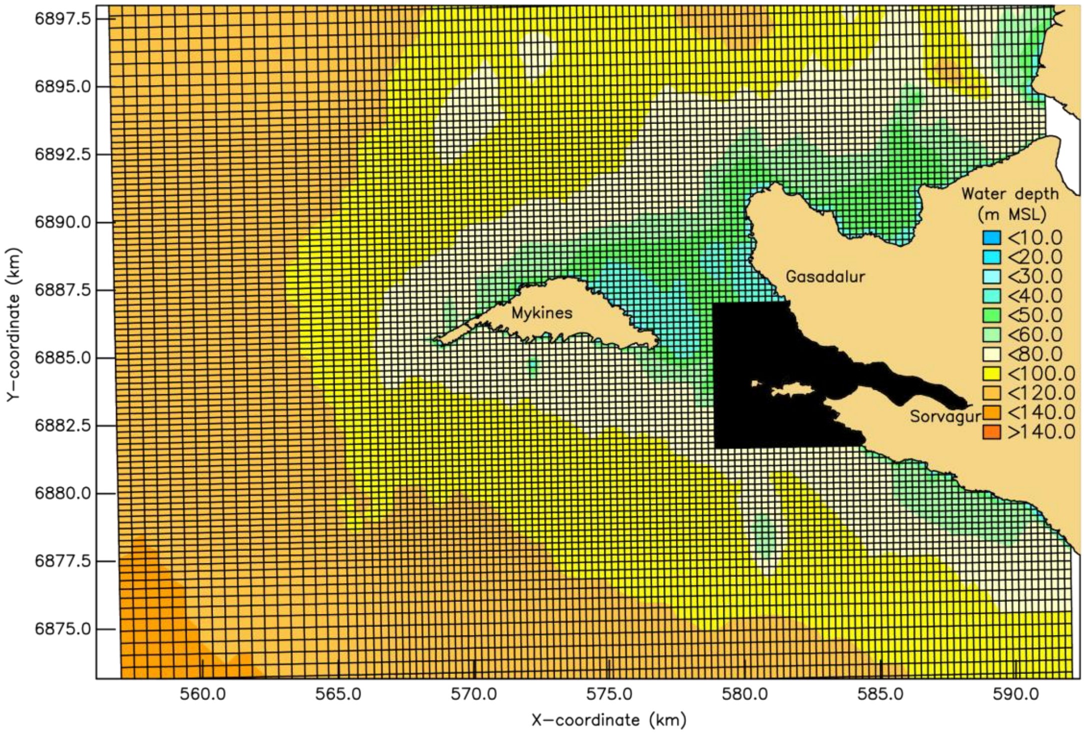

Figure 3.3 The large outer computation grid with its associated bathymetry and the high resolution grid for the fjord.

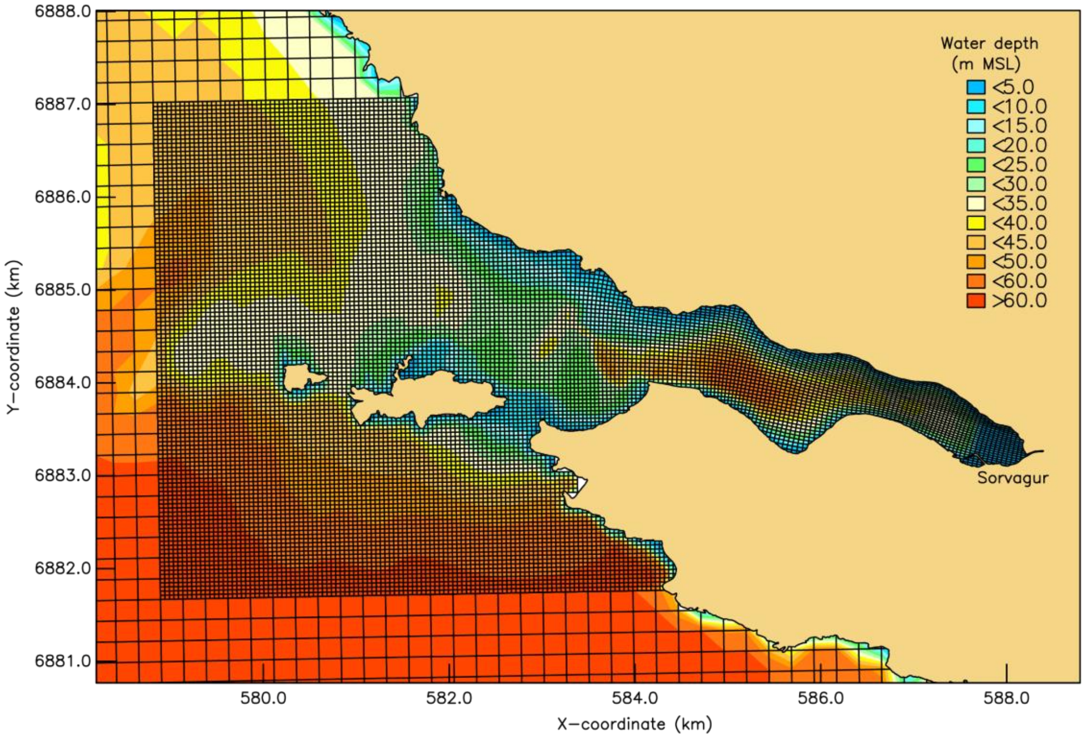

Figure 3.4 The high resolution computational grid for the fjord with the associated bathymetry.

3.1.3 Model set-up: Boundary conditions

There are different types of boundary conditions that can be used for numerical modelling. These depend on the application and availability of data. The smaller fjord model will obtain boundary conditions internally from Delft3D-FLOW online domain decomposition during the simulation process and boundary conditions only need to be specified for the large outer model. These boundary conditions can come from either measurements or output from even larger ocean models. In this case, direct water level measurements are not available along the model boundaries and use was made of model output and satellite altimetry data.

The hydrodynamics of the outer model are driven by water levels, and that is done by specifying so-called tidal constituents. Thirteen tidal constituents were obtained from the TPXO.7.2 tidal model. This is actually a series of global ocean tide models that are continuously corrected by comparing the model to satellite (and other) data (Egbert and Erofeeva, 2002; https://www.tpxo.net/).

The salinity in the model is modelled as a constituent and solved from an advection-diffusion equation. This requires that salinities need to be specified on all the boundaries of the outer model. Daily averaged salinities were obtained from the Copernicus Marine Environment Monitoring Service (CMEMS) through their GLOBAL Ocean Sea Analysis and Forecasting product (CMEMS, 2021). These salinities are not from measurements, but output from the NEMO numerical model (NEMO, 2022).

3.1.4 Model set-up: Surface winds

There are different wind stations located on the Faroe Islands. The winds from the Glyvursnes station operated by Landsverk were used for the large outer domain since at this station the wind is not influenced by the local terrain. The measurements were taken at 70 m above sea level and the magnitudes scaled to 10 m above sea level by the 1/7-rule. The directions were left unchanged. The winds measured at the Vágar Airport wind station operated by the Danish Meteorological Institute (DMI) are considered to be more representative of the winds along the fjord and have been used in the high resolution fjord model. No adjustments were made to the speeds or directions although it may be possible that the wind directions may be altered as wind is channelled along the fjord.

The wind speeds and directions for these two datasets are summarised in the wind roses presented in Figure 3.5. The wind directions are according to the nautical definition i.e relative to true North and positive measured clockwise indicating the direction from which the wind is blowing, where, for example, a wind from East-North-East has a direction of 67.5 degrees. Both stations show strong winds from the West, but the airport winds seem to favour two other directions, namely from the NNW (330 degrees) and from the ESE (120 degrees).

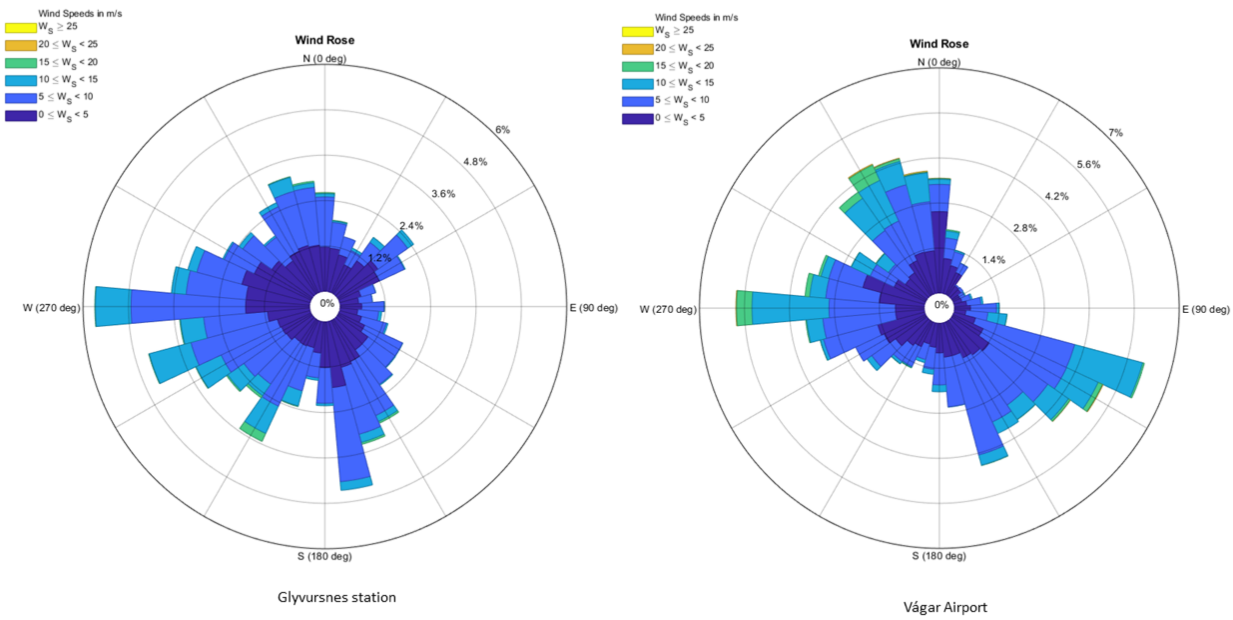

Figure 3.5 Wind speeds and directions from the Glyvursnes station (for the outer model) and from the Vágar Airport (for the fjord model).

3.1.5 Model set-up: Freshwater runoff

There are various locations where the freshwater runoff from the catchment areas flow into Sørvágsfjørður as shown in Figure 3.6. Each runoff river is associated with a certain catchment or drainage area and the magnitude of each area is also shown in Figure 3.6. The average runoff per day has been calculated for each area. The runoff calculations are based on measurements from 1 January 1983 to 31 December 1997 on the island Vágar, where Sørvásfjørður is located.

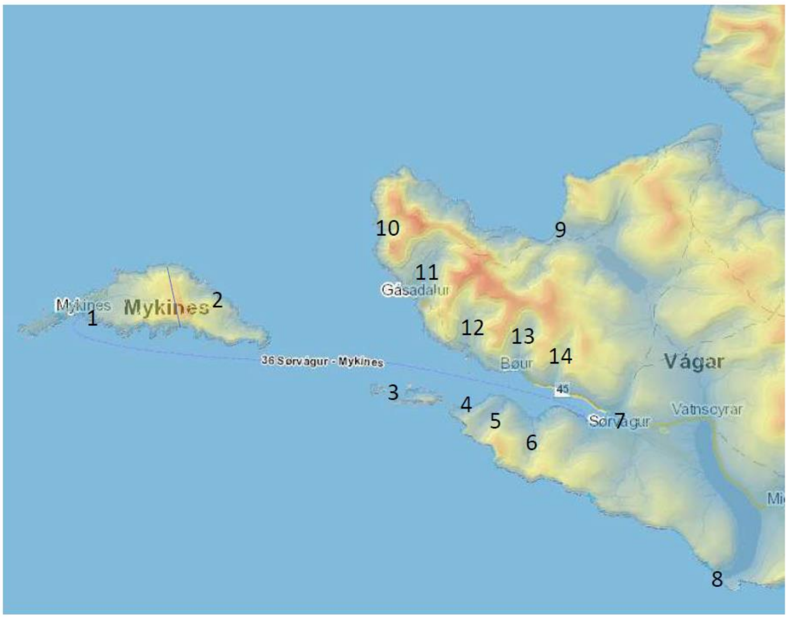

Area	Main river	drainage area (km2)
1	Mykines S	5.437
2	Mykines N	3.835
3	Tindhólmur og Gáshólmur	0.462
4	Múlin	0.421
5	Lambá	1.305
6	Selvíkará	3.512
7	Kirkjuá, Stórá og Skipáir	13.925
8	Bøsdalafossur	34.824
9	Reipsá	35.257
10	Stóragil	2.478
11	Dalsá	6.188
12	Skarðsá	4.739
13	Stórá Bø	3.78
14	Breiðá	3.776

Figure 3.6 Freshwater runoff stations and their estimated drainage areas.

A family of runoff stations have been operational with similar instruments and have been maintained with the same maintenance procedure from 1 January 1983 to 31 December 1997. The runoff stations operated by Landsverk were based on an artificially built runoff profile across a river. A rating curve relating runoff with the measured water levels have been established theoretically or empirically by flow measurements. This data is summarised as daily averaged reduced into a single representative year. The data was scaled by the catchment areas and it was therefore necessary to upscale again to obtain daily average runoff. The daily discharges that are implemented in the model are presented in Figure 3.7.

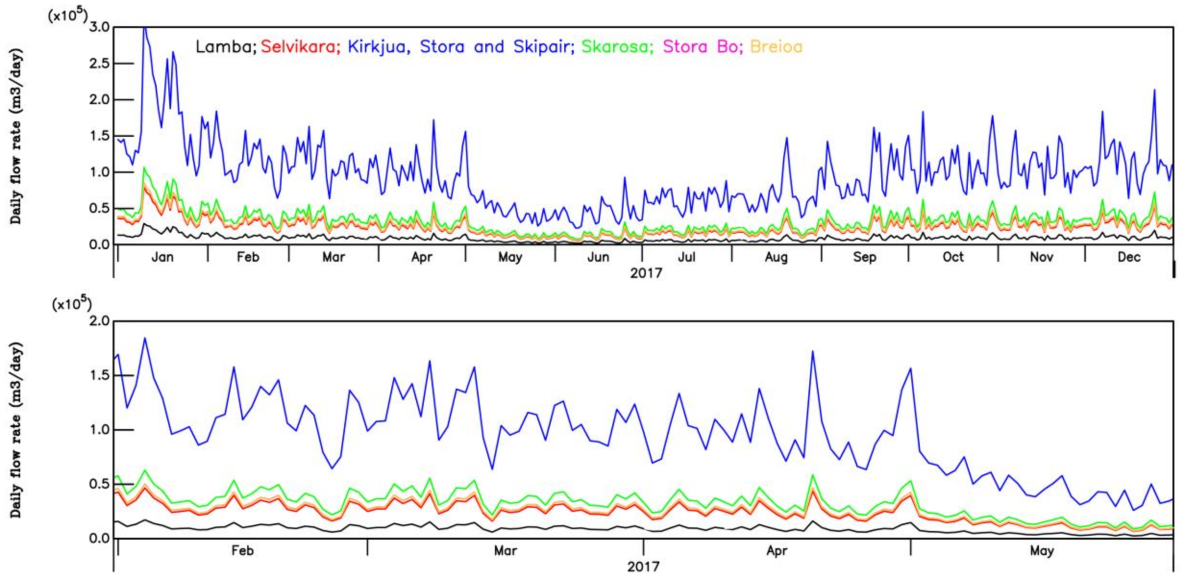

Figure 3.7 Daily freshwater runoff implemented in the model for a year (top panel) and for the simulation months (bottom panel).

3.1.6 Model set-up: Model parameters and settings.

Tidal forcing and salinities were specified at the model boundaries while surface winds were specified over the whole domain and freshwater runoff was implemented as sources. The other notable change is that the default wind drag coefficients were increased by an order of magnitude. Bottom friction is modelled with a Chézy coefficient obtained from the White-Colebrook formulation defined by the Nikuradse roughness length which was set to 0.1 m. Other modelling parameters are provided in Table 3.1.

Table 3.1 Model parameters.

Parameter	Value
Horizontal eddy viscosity and diffusivity	1 m^2/s and 1 m^2/s
Background vertical eddy viscosity and diffusivity	1.0 x 10^{-5} m^2/s and 1.0 x 10^{-5} m^2/s
Wind shear coefficients	0.0011 at 0 m/s and 0.0065 at 100 m/s
Time step	0.25 minute

3.2 Model results

3.2.1 Water levels

Water levels were measured at the ADCP location for the period 7 February 2017 to 1 May 2017. A comparison between the modelled and measured water levels and depths are presented in Figure 3.8. For the majority of February and March the model corresponds well to the hight water amplitudes but underestimates the water levels at ebb tides whereas during April it appears as if the low water amplitudes are calculated correctly while the flood tide amplitudes are underpredicted. This could be due to atmospheric pressure systems or fronts moving through the area which are not included in the model since the tides are only driven by tidal constituents. However, the differences in amplitudes are mostly around 35 cm.

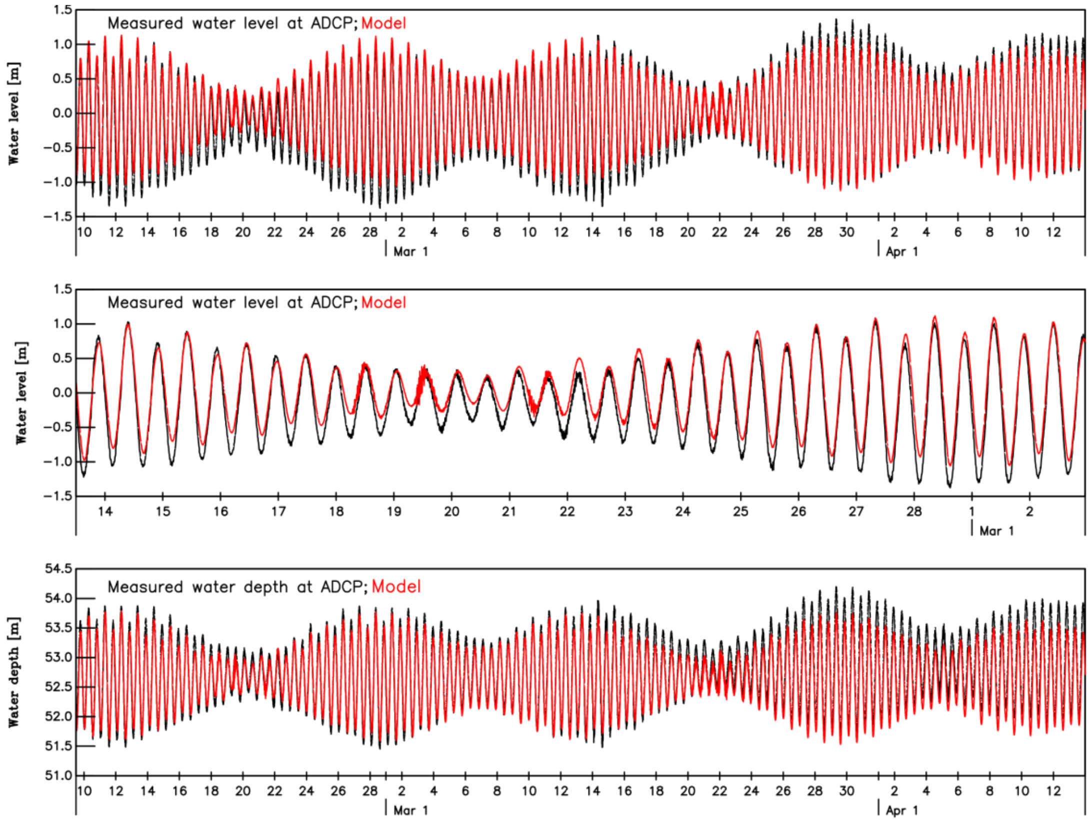

Figure 3.8 Comparison between modelled and measured water levels (top panel) and water depths (bottom panel) for the period 8 February 2017 to 13 March 2017 with a close-up view of water levels (centre panel).

3.2.2 Examples of hydrodynamic results

Examples of the simulated near-surface and bottom currents during the start of an ebb tide and the start of a flood tide are shown in Figures 3.9 to 3.12.

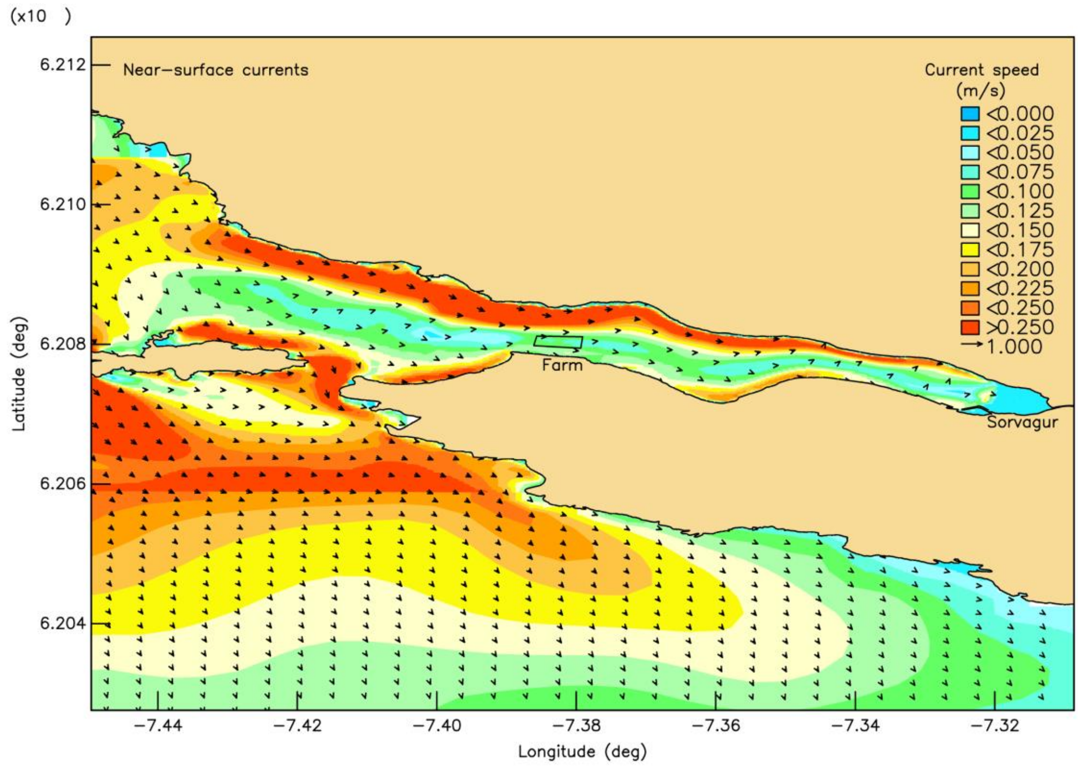

Figure 3.9 Near-surface currents on 20 February 2017 at 16:00 during the start of the ebb tide. The flow is also an example of reverse circulation.

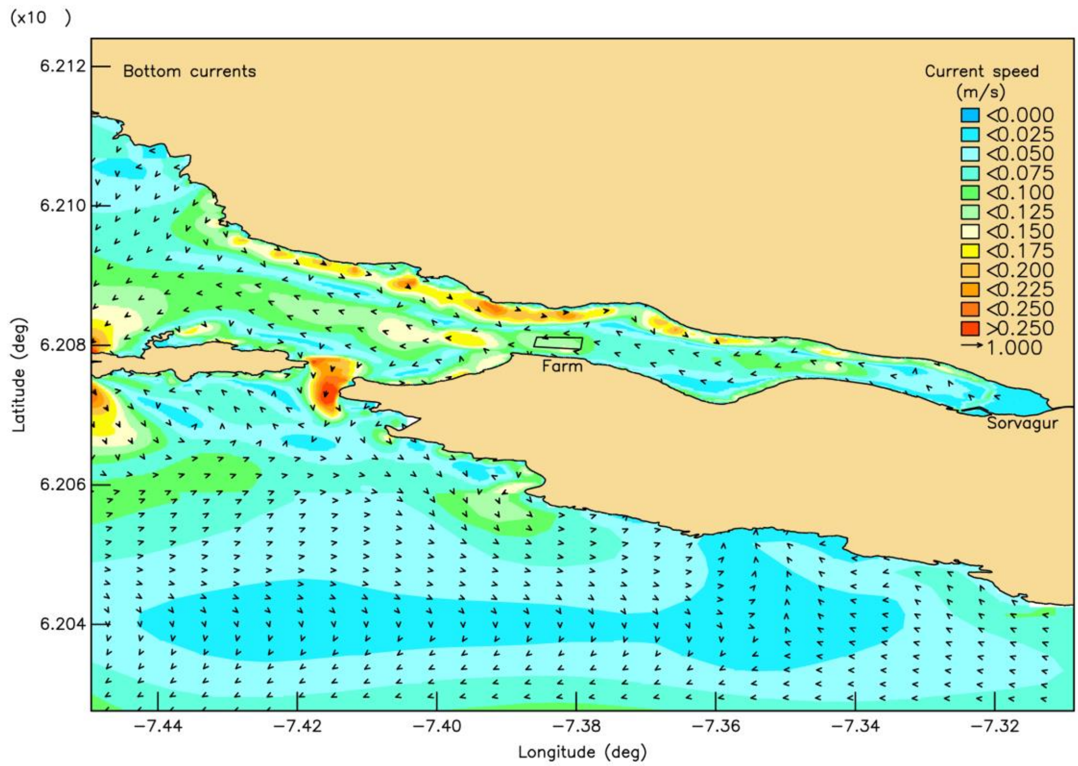

Figure 3.10 Bottom currents on 20 February 2017 at 16:00 during the start of the ebb tide. The flow is also an example of reverse circulation.

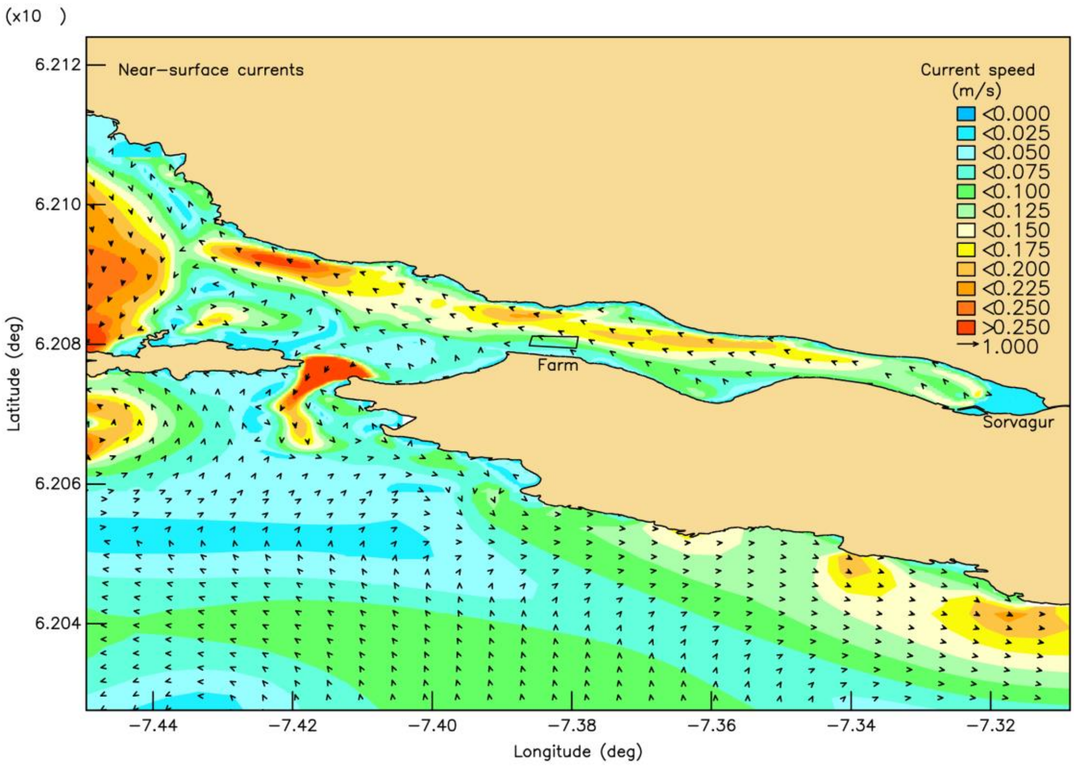

Figure 3.11 Near-surface currents on 6 March 2017 at 08:00 during the start of the flood tide. The flow is also an example of typical estuarine circulation.

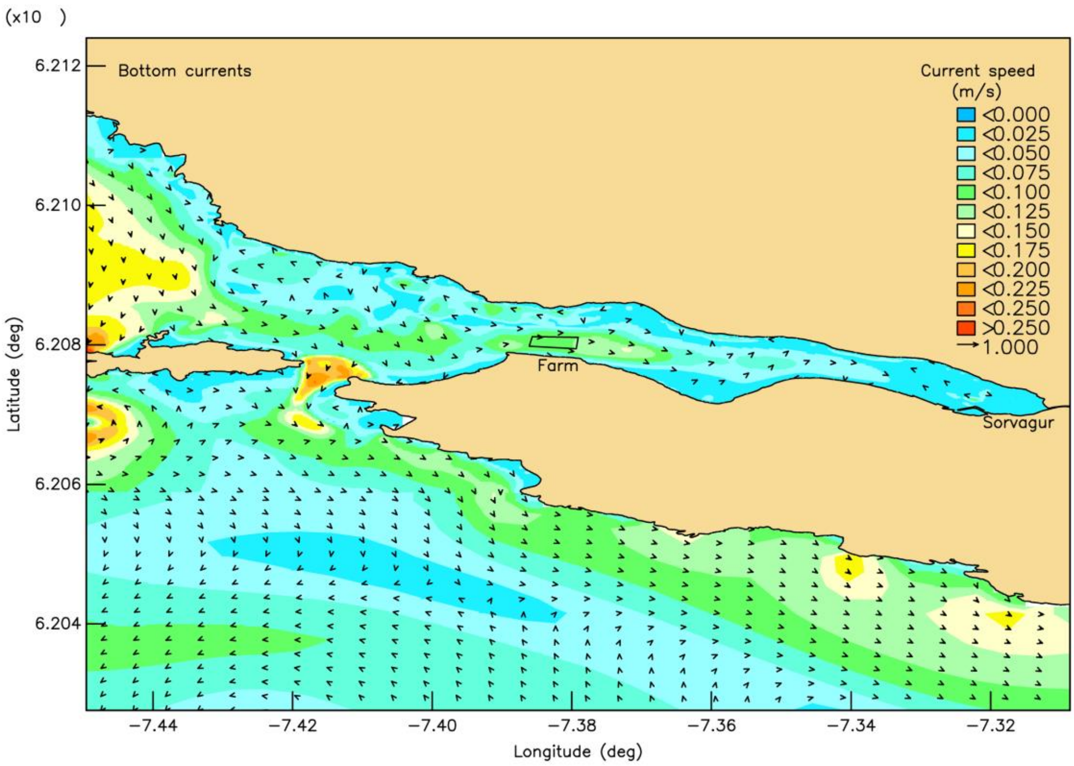

Figure 3.12 Bottom currents on 6 March 2017 at 08:00 during the start of the flood tide. The flow is also an example of typical estuarine circulation.

In these figures (and in general) the currents were stronger in the surface than at the bottom and are stronger on the northern side than on the southern side. Strong cross-currents were calculated outside the lough around the eastern and western sides of Mykines Island.

3.2.3 Comparison of time series results and measurements

Two periods where the model results are compared to the measurements in the near-surface layer and bottom layer are presented in Figure 3.13. Figure 3.13 (top panel) is similar to the measurements presented by á Norði and Patursson (2017) which indicates a period where reverse circulation occurs with surface currents flowing into the fjord due to winds blowing into the fjord. Figure 3.13 (bottom panel) shows the normal estuarine circulation with surface waters moving out of the fjord and more saline water in deeper water flowing into the fjord. These results indicate the model correctly reproduces the correct process although the magnitudes of the modelled currents are smaller than the measurements.

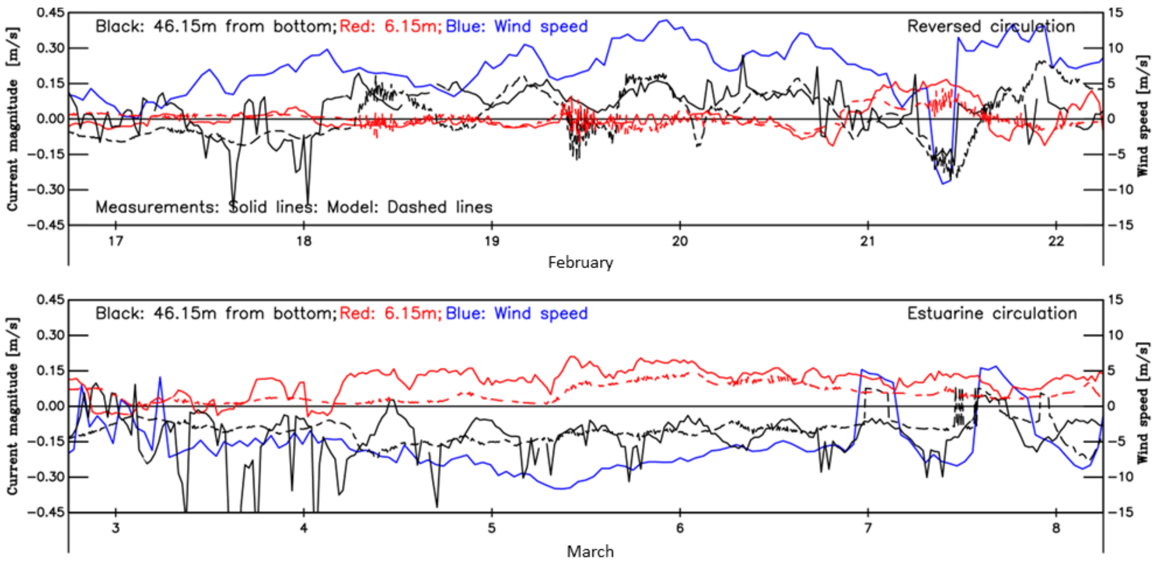

Figure 3.13 Reversed circulation (top panel) with winds continuously directed into the fjord (positive) and estuarine circulation (bottom panel) with winds continuously directed out of the fjord (negative values).

Comparisons of the current speeds and directions at three different depths are presented in Figures 3.14. and 3.15. The speeds at the surface presented in Figure 3.14 are very spiky similar to the data and they do not seem to have a good correspondence with the data. However, at the bottom the model compares well to the data. At mid-depth the current speeds are also similar to the measurements but the model magnitudes are less than those of the measurements. The current directions at all the depths correspond well to the measured directions which is very encouraging.

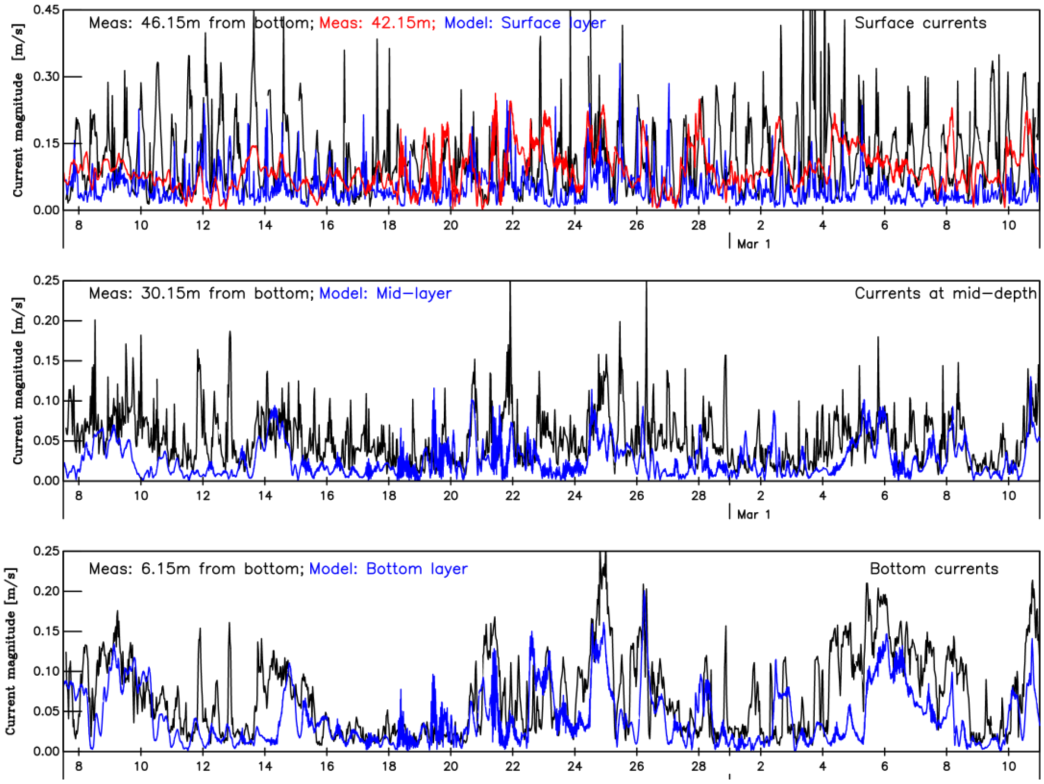

Figure 3.14 Comparison between modelled and measured current speeds at different depths.

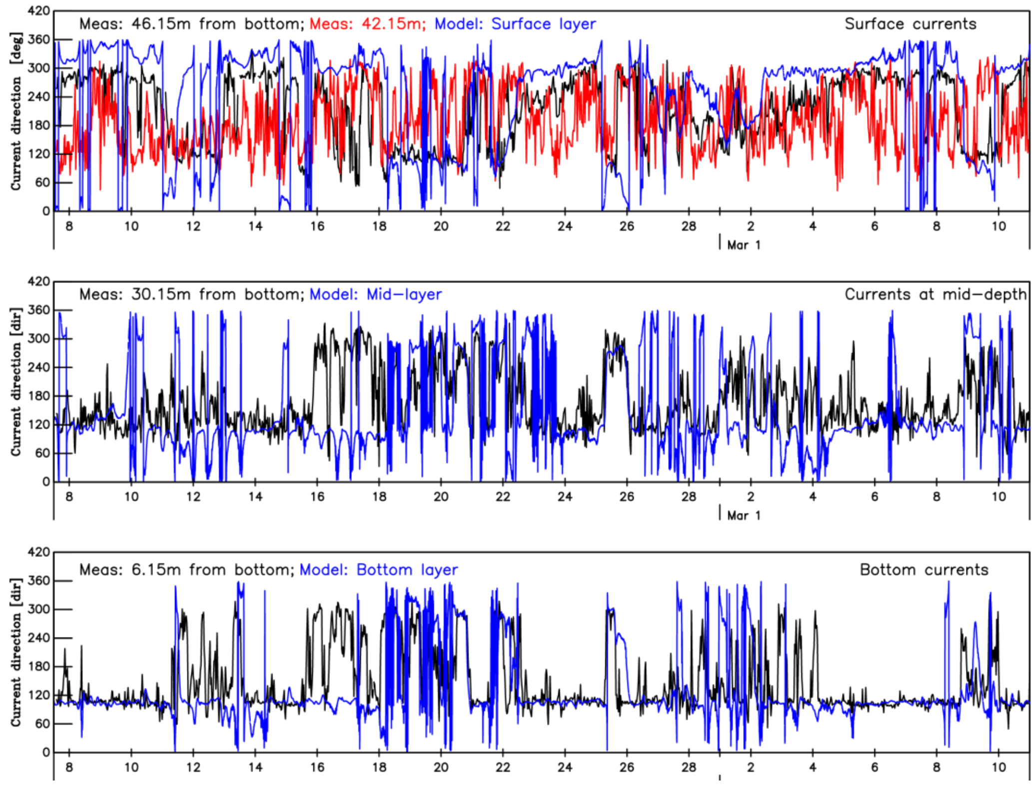

Figure 3.15 Comparison between modelled and measured current directions at different depths.

4. Summary and conclusions

A three-dimensional hydrodynamic model has been developed for Sørvágsfjørður in the Faroe Islands. The model includes the effects of tides, surface winds and freshwater runoff. The model correctly simulates the process of estuarine circulation as well as conditions where reverse circulation occur. Current speeds at the surface are spiky and do not correlate well to the measurements whereas currents at mid-depth and at the bottom show similar behaviour as the measurements although the modelled currents at mid-depth have slightly smaller magnitudes. However, the model is considered adequate to use as research tool to be used in the investigation of various process that depend on the hydrodynamics.

An extension to the model could be to include the simulation of water temperature. For this it is necessary to specify information to simulate air-sea interactions. As a minimum air temperature is required but there are also more sophisticated models that require net solar radiation, humidity and cloud cover as input. Possible improvements of the model can be to specify space-varying wind speeds and pressure. This will allow the effect of passing pressure systems to have an effect on the water levels.

It may be more beneficial to firstly use the modelled results in different ecological models and to improve on the hydrodynamic model only if the results show that improvements are required.

Data availability

The data input to the model was bathymetry, surface winds and freshwater runoff. For model validation tidal and current measurements were used. Bathymetry was obtained from www.kortal.fo, surface winds were from the weather station Glivursnes operated by Landsverk www.landsverk.fo and from the Vágar Airport wind station operated by the Danish Meterological Institute www.dmi.dk. Freshwater runoff was calculated from measurements by Landsverk, and the tide and current measurement was obtained from Hiddenfjrod available at www.envofar.fo; measurement SORD1702 https://mail.fiskaaling.fo/envofar/adcp.

5. References

á Norði, G. and Patursson, Ø. (2017) Estuarine circulation, influenced by weather conditions. Poster available at https://www.fiskaaling.fo/media/2796/fjardarak.pdf

Bannister, R.J., Johnsen, I.A., Hansen, P.K., Kutti, T. and Asplin, L., 2016, *Near- and far-field dispersal modelling of organic waste from Atlantic salmon aquaculture in fjord system*, ICES Journal of Marine Science, doi:10.1093/icesjms/fsw027

CMEMS, 2021, *Product User Manual For the GLOBAL ocean sea physical analysis and forecasting products*, https://resources.marine.copernicus.eu/products.

Cromey, C.J., Nickell, T.D. and Black, K.D., 2002, *TDEPOMOD—modelling the deposition and biological effects of waste solids from marine cage farms,* Aquaculture, 214, pp. 211-239.

Deltares, 2010. *Delft3D-FLOW, Simulation of multi-dimensional flows and transport phenomena, including sediments*, Deltares, User Manual. V.3.14, Delft, the Netherlands.

Hansen, B., Østerhus, S., Hátún, H., Kristiansen, R. and Larsen, K.M.H., 2003, *The Iceland-Faroe inflow of Atlantic water to the Nordic Seas*, Progress in Oceanography, 59, pp. 443-474.

Hansen, B., Poulsen, T., Larsen, K.M.H., Hátún, H., Østerhus, S., Darelius, E., Berx, B., Quadfasel, D. and Jochumsen, K., 2017, *Atlantic water flow through the Faroese Channels*, Ocean Science, 13, pp. 873-888. doi.org/10.5194/os-13-873-2017

Larsen, K.M.H., Hátún, H., Hansen, B. and Kristiansen, R., 2012, *Atlantic water in the Faroe area: sources and variability*, ICES Journal of Marine Science, 69(5), pp. 802-808. doi:10.1093/icesjms/fss028

Lesser, G.P., Roelvink, J.A., van Kester, J.A.T.M. and Stelling, G.S., 2004, *Development and validation of a three-dimensional morphodynamic model*, Coastal Engineering, 51, pp. 883-915.

NEMO, 2021, *NEMO ocean engine*, Scientific Notes of Climate Modelling Center, 27 — ISSN 1288-1619, Institut PierreSimon Laplace (IPSL), doi:10.5281/zenodo.1464816.

Steingrund, P. and Gaard, E. EM, 2008, *Relationships between phytoplankton production and cod production on the Faroe Shelf,* ICES Journal of Marine Science, 62, pp. 163-176. doi:10.1016/j.icesjms.200408019

Symonds, A.M., 2011, *A comparison between far-field and near-field dispersion modelling of fish farm particulate wastes*, Aquaculture Research, 42, pp. 73-85.